Nature of $(C_5Me_5)_2Mo_2O_5$ in water–methanol at pH 0–14. On the existence of $(C_5Me_5)MoO_2(OH)$ and $(C_5Me_5)MoO_2^+$: a stopped-flow kinetic analysis†

Edmond Collange, Juan A. Garcia‡ and Rinaldo Poli*

Laboratoire de Synthèse et d'Electrosynthèse Organométalliques, Université de Bourgogne, Faculté de Science Gabriel, 6 boulevard Gabriel, 21000, Dijon, France.
E-mail: Rinaldo.Poli@u-bourgogne.fr; Fax: +33 (0)3 80 39 60 98
Tel: +33 (0)3 80 39 68 81

Received (in Montpellier, France) 26th February 2002, Accepted 25th April 2002
First published as an Advance Article on the web 12th August 2002

A stopped-flow analysis of compound $Cp^*_2Mo_2O_5$ ($Cp^* = \eta^5$-C_5Me_5) in 20% MeOH–H_2O over the pH range 0–14 has provided the speciation of this molecule as well as the rate and mechanism of interconversion between the various species that are present in solution. The compound is a strong electrolyte in this solvent combination, producing the $Cp^*MoO_2^+$ and $Cp^*MoO_3^-$ ions in equilibrium with a small amount of $Cp^*MoO_2(OH)$, the latter attaining *ca.* 15% relative amount at pH 4. At low pH (< 2.5) $Cp^*MoO_2^+$ is essentially the only species present in solution, while the anion $Cp^*MoO_3^-$ is the dominant species at pH > 6. The acid dissociation constant of $Cp^*MoO_2(OH)$ has been measured directly ($pK = 3.65 \pm 0.02$) while the pK for the protonation equilibrium leading to $Cp^*MoO_3H_2^+$ is estimated as < 0. The three trioxygenated species establish rapid proton transfer equilibria among themselves, but transform to the dioxo species $Cp^*MoO_2^+$ by two slower and independent first-order pathways: loss of H_2O from $Cp^*MoO_3H_2^+$ and loss of OH^- from $Cp^*MoO_2(OH)$. The former pathway is prevalent at pH < 2, where the transformation proceeds to completion, giving rise to kinetics that are first-order in metal and in $[H^+]$. The reverse process is quantitative at pH > 5. The prevalent pathway at high pH is the addition of OH^- to $Cp^*MoO_2^+$, giving rise to kinetics that are first-order in metal and in $[OH^-]$. The kinetics of the equilibration process at intermediate pH are affected by the buffer concentration, indicating a general acid-base catalytic phenomenon. The complete elucidation of the kinetic and thermodynamic scheme was made possible by the combined analyses of the equilibrium in the pH 3–5 range and the kinetics in the extreme pH regions.

High oxidation state organometallic chemistry has experienced a rapid development in the last 20 years, mostly justified by the search for efficient oxidation catalysts. This is exemplified by the numerous studies carried out on the half-sandwich oxo derivatives of rhenium.[1–3] The coordination sphere of high oxidation state metals typically involves electronegative and π-donating ligands such as the halides or negatively charged oxygen-based (oxo, alkoxo) or nitrogen-based (nitrido, imido, amido) ligands. These conditions confer a high degree of covalency to any metal–carbon bond, which consequently becomes quite resistant to hydrolytic conditions. The cyclopentadienyl ligands are perhaps the most compatible organic fragments in this area of organometallic chemistry. It is therefore somewhat surprising that the physical behavior and chemical reactivity of high oxidation state organometallics is not systematically investigated in water, although some of these systems are synthesized in water or by the use of aqueous reagents.

Some of the earliest examples of high oxidation state organometallics are the molybdenum derivatives of general formula $(Ring)_2Mo_2O_5$ (Ring = substituted cyclopentadienyl ligand), first developed in the laboratory of M. L. H. Green for the parent cyclopentadienyl system.[4–6] We have recently reported improved syntheses of the Cp and Cp* compounds ($Cp = \eta^5$-C_5H_5; $Cp^* = \eta^5$-C_5Me_5), and extended them to the preparation of new derivatives containing the sterically congested $C_5HPr^i_4$ and 1,2,4-$C_5H_2Bu^t_3$ rings.[7] The structures of these compounds display neutral dinuclear units with symmetric Mo–(μ-O)–Mo bridges, like the various X-ray structures previously reported for different polymorphs of the Cp* compound.[8–11] A related complex, $Cp^*MoO_3^-$, has been reported independently by the groups of Geoffroy and Sundermeyer.[12–14] These complexes can indeed be prepared in an aqueous medium,[4,7,13–15] but most reported investigations have been restricted to the use of nonaqueous solvents.[8–11,16–19]

We have initiated a research effort aimed at increasing our basic knowledge of the physical properties and chemical reactivity of organomolybdenum compounds in a variety of high oxidation states in water, with the goal of developing new aqueous organometallic chemistry, catalysis and electrocatalysis. In this contribution, we report a thorough study of the Cp^*Mo^{VI} system in an aqueous environment over the entire pH range (0–14). Since compound $Cp^*_2Mo_2O_5$ is insoluble in pure water, while alkali metal salts of $Cp^*MoO_3^-$ (*e.g.*, sodium) are lipophobic, we were forced to carry out our investigation in a mixed MeOH–H_2O solvent. However, the use of just 20% MeOH proved sufficient to keep the neutral compound in solution at sufficient concentrations (up to 4×10^{-4} M) to carry out our UV-visible spectroscopic investigations, while it does not interfere with the aqueous chemistry of the Cp^*Mo^{VI} species as shown by the results obtained.

† Electronic supplementary information (ESI) available: tables of rate constants. See http://www.rsc.org/suppdata/nj/b2/b202106b/

‡ SOCRATES exchange student from the University of Zaragoza.

Experimental

Reagents and solutions

All chemicals were of reagent grade and used as supplied without further purification. HNO_3 and NaOH standard solutions were from Merck–Prolabo Normadoses. The buffers were constituted in single conjugate pairs or in Britton–Robinson (B.R.) mixtures.[20,21] The ionic strength of all solutions was adjusted to 0.1 M by the addition of $NaNO_3$. Compounds $Cp^*_2Mo_2O_5$ and Cp^*MoO_2Cl were prepared according to the literature procedures.[7]

pH and conductivity measurements

The pH of the buffer solutions was determined, at 25 °C, with a Methrom 702 SM pHmeter. The electromotive force of the cell is expressed by the equation $E = E_o - k(\mathrm{pH}) + E_j$.[22] In the presence of supporting electrolyte, such as 0.1 M $NaNO_3$, the junction potential E_j is generally considered as constant in the pH range 2–12.[23–25] The above equation gives $\mathrm{pH} = (E_o - E)/k + E_j/k = \mathrm{pH_{read}} + \Delta\mathrm{pH}$. The slope k (≈59 mV) was obtained by calibration at 25 °C with NBS standard buffers prepared in aqueous medium (0.05 M potassium biphthalate, pH = 4.008; 0.05 M borax, pH 9.196).[26] The correction term, ΔpH, was determined daily by NaOH titration of an HNO_3 solution. It is the difference between the calculated and read pH values obtained in the acidic range. This term was generally close to −0.15 pH units. The pK_s of the mixed solvent (80 : 20 H_2O–MeOH) is the sum of the experimental pH and the calculated pOH values in the basic range.[27] We have obtained $pK_s = 14.25 \pm 0.02$, close to the value determined by Rochester.[25] The electrical conductivity measurements were carried out with a YSI model 35 conductimeter and a Beckman 35 Conductivity Cell.

Stopped-flow kinetic measurements

The stopped flow kinetic runs were carried out with a Hitech SF-61-DX2 apparatus coupled with a Hitech diode-array UV-visible spectrophotometer. Kinetic traces were recorded at 25 °C in the pH range 1–13.25. The cell path length was 1 cm. Two types of manipulations were carried out as follows.

Type 1 experiments (from $Cp^*_2Mo_2O_5$). A 2×10^{-3} M $Cp^*_2Mo_2O_5$ stock solution was prepared in MeOH, since this compound is insoluble in water. For each stopped-flow kinetics run, the $Cp^*_2Mo_2O_5$ solution was prepared by diluting this stock solution with 4 volumes of H_2O to obtain a 20 : 80 (v/v) solvent mixture. This operation was carried out no more than 1 min prior to injection into the stopped-flow cell. When the solution was allowed to stand for a long time (more than half a day) at room temperature, the yellow starting compound reprecipitated. The above solution was mixed in the stopped-flow cell with an equivalent volume of a 20 : 80 (v/v) MeOH–H_2O solution containing NaOH (for the kinetic run at pH ⩾ 11.42) or a buffer at appropriate concentrations (see Results section) for the kinetic runs in the 7–10 pH region.

Type 2 experiments (from $Cp^*MoO_3^-$). A 8×10^{-4} M stock solution of $Na^+Cp^*MoO_3^-$ in 20 : 80 (v/v) MeOH–H_2O was prepared from the MeOH stock solution of $Cp^*_2Mo_2O_5$ by dilution with 4 volumes of a diluted (*ca.* 10^{-3} M) aqueous NaOH solution. This solution was mixed in the stopped-flow cell with an equivalent volume of a 20 : 80 (v/v) MeOH–H_2O solution containing HNO_3 (for the kinetic runs at pH ⩽ 2.30) or a buffer at appropriate concentrations (see Results section) for the kinetic runs in the 2.5–5 pH region.

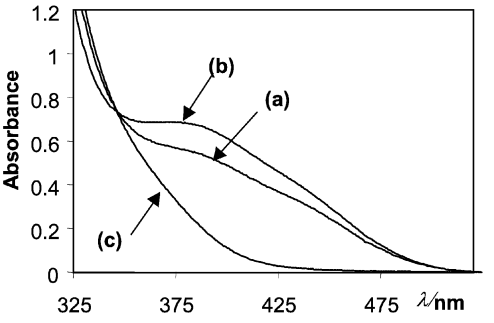

Fig. 1 UV-visible spectra of 20% MeOH–H_2O solutions of (*a*) pure $Cp^*_2Mo_2O_5$(pH *ca.* 4); (*b*) $Cp^*_2Mo_2O_5$ after addition of HNO_3 (pH 1); (*c*) $Cp^*_2Mo_2O_5$ after addition of NaOH (pH = 11.42). All solutions have $[Cp^*_2Mo_2O_5] = 4 \times 10^{-4}$ M.

Data analysis

All kinetic runs were analyzed with the program Specfit[28] while the fitting of the kinetic model to the observed first-order rate constants and equilibrium constants as a function of pH (see Results) was carried out with the Excel Solver. The standard deviations on the determined parameters were obtained by means of the Solver Aid macro.[29]

Results and discussion

(a) Kinetic study of the anation reaction of $Cp^*_2Mo_2O_5$

Solutions of $Cp^*_2Mo_2O_5$ in 20% MeOH–H_2O are yellow and display an absorption spectrum that is characterized by a strong band in the UV with two shoulders at *ca.* 390 and 440 nm as shown by the trace *a* of Fig. 1. The observed pH for this solution is *ca.* 4. This spectrum is qualitatively identical but has a lower intensity than that recorded on the same solution after lowering the pH to 1 by the addition of a strong acid (HNO_3), see trace *b* of Fig. 1. The reason for this phenomenon will become apparent after we have examined in detail the kinetics in the entire pH range (section d). When NaOH is added to the starting solution, on the other hand, this became essentially colorless, see trace *c* of Fig. 1. The latter change is attributed to the formation of the previously described anion $Cp^*MoO_3^-$.[12–14] This solution turns back to yellow if, at this point, the pH is lowered again. The kinetics of this acidification process will be examined in detail in the next section. All spectral changes witnessed during this investigation as a function of pH are perfectly reversible with no loss of intensity, indicating that all transformations are analytically clean.

The anation of $Cp^*_2Mo_2O_5$ has been investigated by stopped-flow kinetics with UV-visible detection in the basic pH range by using NaOH solutions at different concentrations (pH 11.42–13.25) or buffers at pH < 11. In all cases, the final spectrum is identical to that shown in Fig. 1 (trace *c*), showing that the transformation into the anionic complex $Cp^*MoO_3^-$ proceeds to completion under these conditions. All tranformations obey precise first-order kinetics and the log of the observed rate constant (k_{+obs}) varies linearly with the pH (slope 1) for the pH > 11 data, as shown in Fig. 2. This demonstrates that the slow step has a first-order dependence on the concentration of OH^-. All k_{+obs} values can be found in the Electronic supplementary information (ESI). The behavior at pH < 11 will be analyzed in section h.

The rate law of this transformation could in principle be easily interpreted on the basis of a rate determining attack of OH^- on the dinuclear $Cp^*_2Mo_2O_5$ complex, the nucleofuge being the $Cp^*MoO_3^-$ anion. The resulting product of nucleophilic exchange, the conjugate acid $Cp^*MoO_2(OH)$, would be immediately deprotonated under these pH conditions. The p*K*

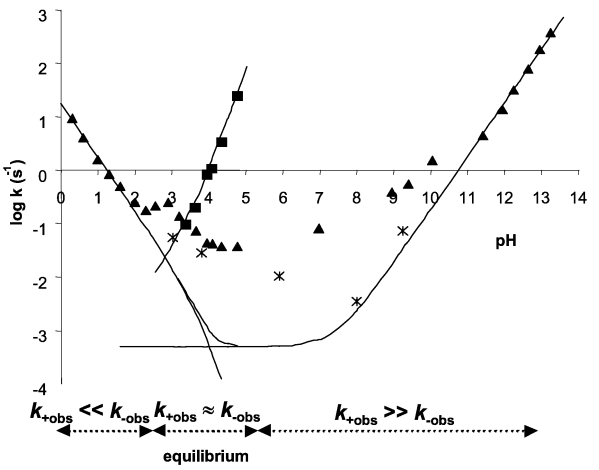

Fig. 2 Plot of the experimental log k_{obs} (triangles) and log K_{eq} (squares) *vs.* pH. The curves drawn correspond to the best fit (k_{obs}, k_{+obs}, k_{-obs} and K_{eq}) according to the equations given in the Results section. Stars correspond to the k_{obs} values extrapolated to zero buffer concentration. All solutions have $[Cp^*_2Mo_2O_5] = 4 \times 10^{-4}$ M.

study of the $Cp^*MoO_2(OH)/Cp^*MoO_3^-$ couple, shown in the next section, confirms the validity of this statement. It will be shown later, however, that the given mechanistic interpretation is incorrect.

(b) Protonation of $Cp^*MoO_3^-$: formation of $Cp^*MoO_2(OH)$ and p*K* study

A stock solution of $Cp^*MoO_3^-$ in 20% MeOH–H_2O was prepared by adding the minimum excess amount of NaOH to a $Cp^*_2Mo_2O_5$ solution prepared as described above, in order to adjust the pH to around 8–9. This was then mixed in the stopped-flow apparatus with various strong acid or buffer solutions, obtaining a final acidic pH. The UV-visible monitoring indicated an immediate change of the spectrum when the final pH was < 6, followed by a slower spectral evolution. We interpret this behavior as the result of an immediate protonation yielding $Cp^*MoO_2(OH)$ (proton transfer reactions are generally diffusion-controlled), which then evolves further. The implication of $Cp^*MoO_2(OH)$ during the protonation of $Cp^*MoO_3^-$, ultimately leading to the dinuclear complex $Cp^*_2Mo_2O_5$, has already been proposed but no spectroscopic evidence for the existence of this compound was reported.[14] Reactions of $Cp^*MoO_3^-$ with other electrophiles Y^+, on the other hand, have allowed the isolation of stable $Cp^*MoO_2(OY)$ complexes, for instance with $Y = Si(CH_2Ph)_3$.[19] The same transformation occurs for the tungsten analog.

The p*K* value for the acid dissociation of $Cp^*MoO_2(OH)$ has been obtained from the analysis of the first spectrum (recorded within 1 ms from the time of mixing) as a function of pH, see Fig. 3. The solutions buffered at pH > 6 showed essentially the unaltered spectrum of $Cp^*MoO_3^-$, whereas the solutions buffered at pH < 2 showed essentially the same spectrum, which is attributed to $Cp^*MoO_2(OH)$. A SPECFIT[28] global analysis yields $pK = 3.65 \pm 0.02$ for the acid dissociation constant.

(c) Kinetic analysis of the $Cp^*MoO_2(OH)$ evolution at pH $\leqslant 2$

After the quantitative transformation of $Cp^*MoO_3^-$ to its conjugate acid in the stopped-flow apparatus, the spectrum evolved, ultimately yielding a pH independent final spectrum (at pH < 2), showing a quantitative transformation under these conditions. Fig. 4 shows an example at pH 1. It is to be noted that this final spectrum (trace *b*) corresponds to trace *b* of Fig. 1 and not to the spectrum of the starting $Cp^*_2Mo_2O_5$ solution (trace *a* of Fig. 1). Thus, the final product obtained from $Cp^*MoO_2(OH)$ under these conditions *is not the dinuclear species*.

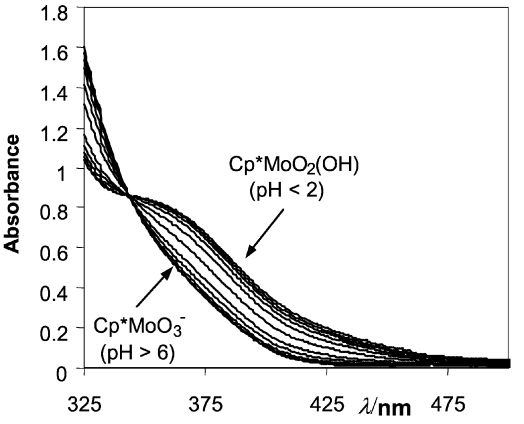

Fig. 3 Spectra in 20% MeOH–H_2O of solution obtained by acidification of $Cp^*MoO_3^-$ at different pH values and recorded immediately (*ca.* 1 ms) after mixing. All initial solutions have $[Cp^*MoO_3^-] = 8 \times 10^{-4}$ M.

All kinetics are first-order in metal and give rise to the observed rate constants k_{-obs} reported in the ESI. These rate constants depend on the pH as shown in Fig. 2. The slope of the log k_{-obs} *vs.* pH is -1, namely the reaction is first-order with respect to $[H^+]$. On the basis of this observation, it is relatively straightforward to propose that $Cp^*MoO_2(OH)$ undergoes a rapid and reversible protonation equilibrium to afford a $Cp^*MoO_3H_2^+$ intermediate, which then decomposes in a slow rate-determining step.

(d) Kinetics in the equilibrium range

The above studies have shown that a quantitative conversion to $Cp^*MoO_3^-$ occurs at pH > 7 while a quantitative conversion to a new species occurs at pH $\leqslant 2$.[30] Adjusting the pH at intermediate values, starting from either a $Cp^*MoO_3^-$ or a $Cp^*_2Mo_2O_5$ solution, led to the evolution to a different and pH-dependent equilibrium situation. An example at pH 4.06 is shown in Fig. 5. Trace *a* is the first recorded spectrum starting from the $Cp^*MoO_3^-$ solution and corresponds therefore to the acid dissociation equilibrium mixture of $Cp^*MoO_3^-$ and $Cp^*MoO_2(OH)$. This solution evolves toward the equilibrium solution (trace *c*) following *first-order kinetics*.

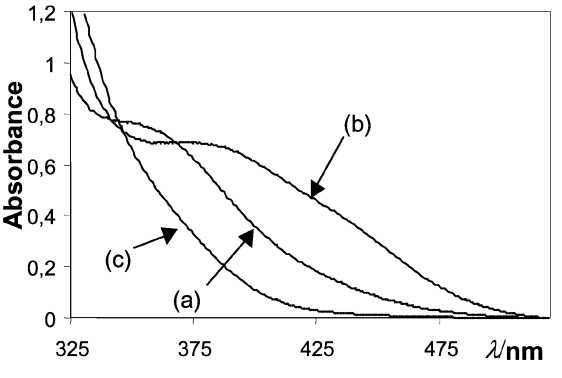

Fig. 4 Key UV-visible spectra for the $Cp^*MoO_2(OH)$ evolution at pH 1 in 20% MeOH–H_2O. (*a*) Initial spectrum (*ca.* 1 ms after mixing). (*b*) Final spectrum. (*c*) Spectrum of $Cp^*MoO_3^-$. All initial solutions have $[Cp^*MoO_3^-] = 8 \times 10^{-4}$ M.

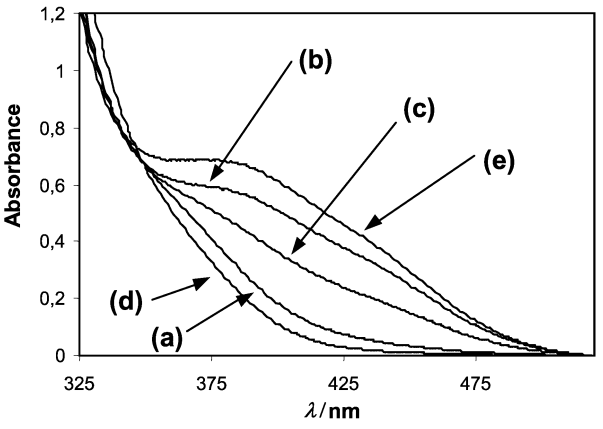

Fig. 5 Key UV-visible spectra for the evolution of $Cp^*MoO_3^-$ and $Cp^*_2Mo_2O_5$ at pH 4.08 in 20% MeOH–H_2O. (*a*) Initial spectrum from the $Cp^*MoO_3^-$ solution (*ca.* 1 ms after mixing). (*b*) Initial spectrum from the $Cp^*_2Mo_2O_5$ solution (*ca.* 1 ms after mixing). (*c*) Equilibrium spectrum. (*d*) Reference spectrum at pH 11.35. (*e*) Reference spectrum at pH 1.

Trace *b* is the first recorded spectrum starting from the $Cp^*_2Mo_2O_5$ solution (the true nature of which will be revealed in the next paragraph). This solution evolves to the *same* equilibrium solution (trace *c*), following again *first-order kinetics*. At each investigated pH value, starting from either solution yielded the *same equilibrium spectrum with identical observed first-order rate constants* (within experimental error), provided that *the same buffer concentration* was used for both experiments, see section h. All individual values of the observed rate constants (k_{obs}) can be found in the ESI.

The results of the kinetics investigations in the equilibrium region demonstrate that compound $Cp^*_2Mo_2O_5$ does not maintain its molecular, dinuclear nature in the 20% MeOH–H_2O solution. Under the assumption that this species is indeed present and transforms to the anion by a first-order process as seen in section a, the microscopic reverse, which becomes observable in the equilibrium region, *should* have a second-order dependence on the metal concentration. This situation occurs, for instance, for the equilibration between mononuclear $HMoO_3^+$(aq) and dinuclear $H_2Mo_2O_6^{2+}$ (aq).[31] However, this is not the case for our Cp^*Mo^{VI} system. This is further confirmed by the little or no dependence of the measured rate on the metal concentrations for the same pH value (data are available in the ESI). The strictly first-order behavior observed *for all transformations at all pH values* forces us to conclude that only mononuclear species are involved.

(e) Nature of the low pH species and nature of $Cp^*_2Mo_2O_5$ in 20% MeOH–H_2O

As seen above, the acidification of $Cp^*MoO_3^-$ immediately affords $Cp^*MoO_2(OH)$, which decays (quantitatively at pH < 3) to a new species with a rate law showing a first-order dependence on the proton concentration. This behavior is interpreted as resulting from a fast and reversible protonation of $Cp^*MoO_2(OH)$ to afford a $Cp^*MoO_3H_2^+$ intermediate, which then slowly evolves to a final product, now known to be mononuclear. It is straightforward to propose that the slow step corresponds to dissociation of a water ligand, leading to the cationic complex $Cp^*MoO_2^+$, see Scheme 1,[32] which would therefore correspond to the dominant species at pH < 2. We shall now present further evidence confirming the presence of this cationic species before returning to the kinetic scheme.

The implication of the above proposition and of Scheme 1 is that the dinuclear complex $Cp^*_2Mo_2O_5$ ionizes in the 20% MeOH–H_2O solution to initially produce a 1 : 1 mixture of the $Cp^*MoO_2^+$ and $Cp^*MoO_3^-$ ions, as in eqn. (1):

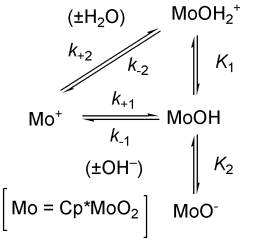

Scheme 1

$$Cp^*_2Mo_2O_5(s) \rightleftharpoons Cp^*_2Mo_2O_5(solv) \rightleftharpoons Cp^*MoO_2^+(solv) + Cp^*MoO_3^-(solv) \quad (1)$$

Indeed, the spectrum of a $Cp^*_2Mo_2O_5$ solution in Fig. 1 (trace *a*) is quite close to a linear combination of the $Cp^*MoO_2^+$ spectrum (trace *b*) and that of $Cp^*MoO_3^-$ (trace *c*).[33] The ionic nature of $Cp^*_2Mo_2O_5$ in 20% MeOH–H_2O is confirmed by electrical conductivity studies, as shown in Fig. 6. Under the validity of eqn. (1), we wondered whether the known Cp^*MoO_2Cl complex would also ionize in the same medium [see eqn. (2)]. The conductivity study of solutions of this compound fully confirms this hypothesis (Fig. 6).

$$Cp^*MoO_2Cl(s) \rightleftharpoons Cp^*MoO_2Cl(solv) \rightleftharpoons Cp^*MoO_2^+(solv) + Cl^-(solv) \quad (2)$$

Although qualitatively quite convincing, the conductivity data present some unusual features from the quantitative point of view. The molar conductivity values vary more or less linearly with $[Cp^*_2Mo_2O_5]^{1/2}$ or $[Cp^*MoO_2Cl]^{1/2}$ for concentrations greater than 4×10^{-5} M, as expected for strong electrolytes. However, they are very large and the slopes of these lines are greater than expected for the low concentration range explored in our case (typical salts have an almost negligible variation in this range). Moreover, the linearity is lost at lower concentrations, and the molar conductivities at infinite dilutions are very large ($> 300 \times 10^{-4}$ Ohm^{-1} m^2 mol^{-1}). Other 1 : 1 organic salts show conductivities in the range $(80–115) \times 10^{-4}$ Ohm^{-1} m^2 mol^{-1} in pure methanol for 10^{-3} M solutions.[34] Infinite dilution values are rarely above 150 for 1 : 1 salts except when hydronium ions are involved. All these features will in fact turn out to be completely consistent with our model. However, their full rationalization requires that we first detail the speciation of Cp^*Mo^{VI} in the entire pH range (section g).

Compound $Cp^*_2Mo_2O_5$ is soluble in all common organic solvents and essentially insoluble in pure water. This indicates

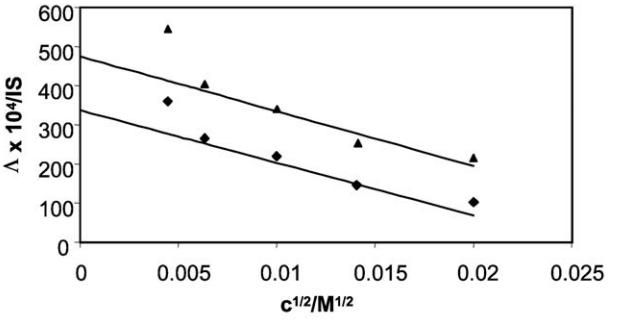

Fig. 6 Molar conductivity of a 20% MeOH–H_2O solution of $Cp^*_2Mo_2O_5$ (diamonds) or Cp^*MoO_2Cl (triangles) as a function of concentration. The lines are a linear fit.

Table 1 Molar conductivities for 4×10^{-4} M solutions of $Cp^*_2Mo_2O_5$ in different solvents

Solvent	Λ^a /Ohm^{-1} m^2 mol^{-1}
MeCN	0[b]
CH_2Cl_2	0
EtOH	0.4
Acetone	0.8
MeOH	4.2
20% MeOH–H_2O	102

[a] Corrected for the molar conductivity of the pure solvent. [b] In this solvent, the measured conductivity was smaller for the solution than for the pure solvent.

that the left hand side equilibrium of eqn. (1) (dissolution of molecular $Cp^*_2Mo_2O_5$) is highly sensitive to the hydrophobic nature of the molecule. However, the right hand side equilibrium of eqn. (1) is highly sensitive to the dielectric constant. This view is confirmed by the comparison of the molar conductivities in different solvents at a 4×10^{-4} M concentration, see Table 1. Thus, the water-rich solvent mixture used in this study favors an essentially complete ionization.

(f) The complete scheme

For convenience, the formulas of complexes $Cp^*MoO_3^-$, $Cp^*MoO_2(OH)$ and $Cp^*MoO_2^+$ will be heretofore abbreviated as MoO^-, MoOH and Mo^+, respectively. The kinetic results described in sections a and b can now be reinterpreted according to Scheme 1, ultimately allowing us to understand and rationalize the kinetic and thermodynamic behavior of the Cp*Mo system in the entire pH range. The vertical transformations on the right hand side of the scheme are simple protonation/deprotonation equilibria and are rapid (probably diffusion-limited) on the time scale of the stopped-flow experiments. They can therefore be considered as a single species [abbreviated as *MO*, see eqn. (3)] for kinetic purposes.

$$[MO] = [MoO^-] + [MoOH] + [MoOH_2^+] \quad (3)$$

The kinetic evolution of the system under any pH condition can therefore be treated as a reversible first-order equilibration between complex Mo^+ on one side and the species *MO* (the intimate nature of which is pH dependent) on the other side. The development of the kinetic scheme affords eqn. (4) for the overall rate constant for the loss of oxygen-containing species (water and OH^-) and eqn. (5) for the overall rate of the uptake of oxygen-containing species.

$$k_{+obs} = k_{+2} + k_{+1}K_s[H^+]^{-1} \quad (4)$$

$$k_{-obs} = \frac{k_{-1} + k_{-2}K_1^{-1}[H^+]}{K_1^{-1}[H^+] + 1 + K_2[H^+]^{-1}} \quad (5)$$

The observed rate constant (k_{obs}) is then simply given as the sum of k_{+obs} and k_{-obs}. The k_{+obs}/k_{-obs} ratio, on the other hand, gives an operational equilibrium constant K_{eq}, which will be pH dependent. This constant corresponds to the ratio between the sum of all oxygenated species (*MO*) and the non-oxygenated species Mo^+.

On the basis of this scheme, it is now possible to see that the acidification of MoO^-/MoOH leads to Mo^+ by two different pathways, namely loss of OH^- from MoOH and loss of water from $MoOH_2^+$, the latter predominating at low pH. The pK_2 value (3.65 ± 0.02) is available from the studies described in section b, thus the term $K_2[H^+]^{-1}$ in the denominator of eqn. (5) is negligible at pH < 3. The protonation of MoOH does not occur to a significant extent down to pH 0. This is clearly shown by the study in Fig. 2, provided that $MoOH_2^+$ does not have a spectrum perfectly identical to that of MoOH. This means that $pK_1 \ll 0$ and the term $K_1^{-1}[H^+]$ in the denominator of eqn. (5) is also negligible. Under these conditions, eqn. (5) simplifies to the rate law $k_{-obs} = k_{-1} + (k_{-2}/K_1)[H^+]$, or $k_{-obs} = (k_{-2}/K_1)[H^+]$ when loss of water from species $MoOH_2^+$ predominates, as at low pH. Indeed, this is the observed trend. Since $pK_1 < 0$, individual values of k_{-2} and K_1 cannot be obtained. Fitting the simplified rate law to the experimental data gives $k_{-2}/K_1 = 17.26 \pm 0.22$ s^{-1}.

The reverse process (conversion of Mo^+ to MoOH/MoO^-) takes place by the microscopic reverse of the two pathways mentioned above, namely nucleophilic addition of either H_2O (k_{+2}) or OH^- (k_{+1}) to Mo^+. The expression of eqn. (4) shows that the latter pathway will prevail at high pH, giving rise to a first-order dependence on [OH^-], as experimentally observed. Fitting eqn. (4) to the experimental data gives $k_{+1} = (3.26 \pm 0.04) \times 10^3$ s^{-1} M^{-1}. In order to elucidate the complete scheme, two rate constants are still missing: k_{-1} and k_{+2}. However, these are linked to each other by the thermodynamic cycle of Scheme 1, as shown by eqn. (6):

$$\frac{k_{+1}}{k_{-1}}K_s = \frac{k_{+2}}{k_{-2}}K_1 \quad (6)$$

The operational equilibrium constant, K_{eq}, can therefore be expressed as in the simplified eqn. (7), since pH > pK_1 over the entire pH range (*vide supra*).

$$K_{eq} = \frac{k_{+1}K_s}{k_{-1}[H^+]}\left(1 + \frac{K_2}{[H^+]}\right) = \frac{k_{+2}K_1}{k_{-2}[H^+]}\left(1 + \frac{K_2}{[H^+]}\right) \quad (7)$$

In principle, the missing parameter may be obtained in two independent ways. The first one is *via* the rate of equilibration in the intermediate region and subsequent fitting of k_{obs} to the sum of eqns. (4) and (5). The second one is *via* the measurement of the pH-dependent equilibrium [*MO*]/[Mo^+] and fitting of eqn. (7). The first method cannot be applied since the equilibration rates are affected by a general acid/base catalysis in the buffered pH region (*vide infra*). The second method is described in the next section.

(g) The equilibrium in the intermediate pH range

The kinetic analyses in the extreme pH regions (< 2 and > 6) have provided us with the individual spectra of the pure species Mo^+, MoOH and MoO^-, see above. We are therefore in a position to deconvolute the equilibrium spectrum obtained for the kinetic runs at each pH into the sum of the spectra of the above individual species. This operation is conveniently carried out with the program SPECFIT[28] and is facilitated by the independent knowledge of the [MoO^-]/[MoOH] ratio from the pK_2 value. An excellent fit to the equilibrium spectrum was obtained at each pH value between 3 and 5. Outside this range, the equilibrium is too shifted to either side, that is Mo^+ or the MoOH/MoO^- mixture (*MO*), to obtain any meaningful information. The experimental values of the *MO*/[Mo^+] ratio are shown in Fig. 2 together with the best fit given by eqn. (7). It is to be noted that the K_{eq} curve has a transition from slope 1 to slope 2 in correspondence to the pK_2 value. The fit of eqn. (7) provides the individual values of $k_{-1} = (6.32 \pm 0.03) \times 10^{-7}$ s^{-1} and $k_{+2} = (5.01 \pm 0.12) \times 10^{-4}$ s^{-1}. At this point, feeding all known rate and acidity constants into eqns. (4) and (5) (the $K_2/[H^+]$ term in the denominator of this equation is neglected) provides the calculated curves shown in Fig. 2.

From all derived rate and acidity constants (summarized in Table 2), it is now possible to obtain the detailed speciation of the Cp^*Mo^{VI} system at all pH values. The relative proportion of *MO* and Mo^+ is given by eqn. (7) and the relative proportion of species MoOH and MoO^- is provided by the pK_2

Table 2 Summary of all rate and equilibrium constants (Scheme 1)

pK_1	< 0
pK_2	3.65 ± 0.02
k_{+1}	$(3.26 \pm 0.04) \times 10^3$ M^{-1} s^{-1}
k_{-1}	$(6.32 \pm 0.03) \times 10^{-7}$ s^{-1}
k_{+2}	$(5.01 \pm 0.12) \times 10^{-4}$ s^{-1}
k_{-2}/K_1	17.26 ± 0.22 s^{-1}

expression. Species $MoOH_2^+$ can be neglected. The result is graphically shown in Fig. 7. According to this result, Mo^+ is essentially the only species in solution at pH < 2.5 while MoO^- is the dominant species at pH > 6. All species, including MoOH, are simultaneously present in the intermediate pH range. The maximum relative concentration of MoOH (*ca.* 15%) will be present at pH ≅ 4.

It now becomes evident that, upon dissolution in 20% MeOH–H_2O, $Cp^*_2Mo_2O_5$ will provide equivalent amounts of Mo^+ and MoO^- and a small amount of MoOH, while the pH will self-regulate around 4.0 by hydrolysis of part of the Mo^+, provided the solutions are sufficiently concentrated ($> 10^{-3}$ M). For more dilute solutions, a greater proportion of Mo^+ hydrolyzes to afford MoO^- and twice the same amount of protons. A similar behavior occurs when the Mo^+ species is generated by the ionization of Cp^*MoO_2Cl. The concentrations of the different species H^+, OH^-, Mo^+, MoOH and MoO^- can be calculated in a straightforward fashion from all known equilibrium constants. The results are presented in Fig. 8.

At this point, we can analyze again and correctly interpret the results of the electrical conductivity study shown in Fig. 6. In order to fit the conductivity data, the molar conductivities, λ_+ or λ_-, of every ionic species at each concentration were considered identical to the value λ^0_+ or λ^0_- at infinite dilution. This is a reasonable hypothesis given our small concentrations ($< 8 \times 10^{-4}$ M). In addition, the values of λ^0_{H+} and λ^0_{Cl-} were fixed to the literature values (228.8×10^{-4} and 48×10^{-4} S mol^{-3} m^3, respectively)[35] as all attempts to keep them as free parameters led to instability. A global fitting of both $Cp^*_2Mo_2O_5$ and Cp^*MoO_2Cl curves with common molar conductivities yielded a very good agreement between the experimental and calculated curves according to our kinetic and thermodynamic scheme (see Fig. 9). The values of λ^0_{Mo+} and λ^0_{MoO-} provided by the fit are $(72 \pm 6) \times 10^{-4}$ and $(39 \pm 10) \times 10^{-4}$ S mol^{-3} m^3, respectively. These two values are in a reasonable range and are relatively close to each other, as one might expect from the similar size of the two ions. The determination of these values with a higher precision is prevented by the limited solubility of the compound and by the small contribution of these ions to the electrical conductivity at low concentrations in the presence of a significant amount of the more mobile protons.

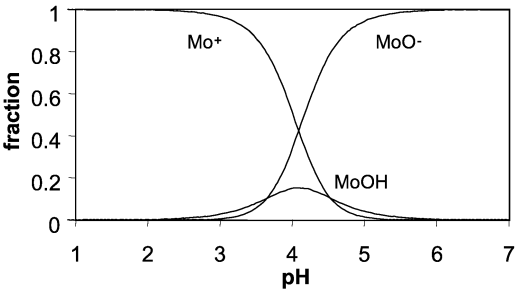

Fig. 7 Relative proportion of species Mo^+, MoOH and MoO^- at all pH values in 20% MeOH–H_2O.

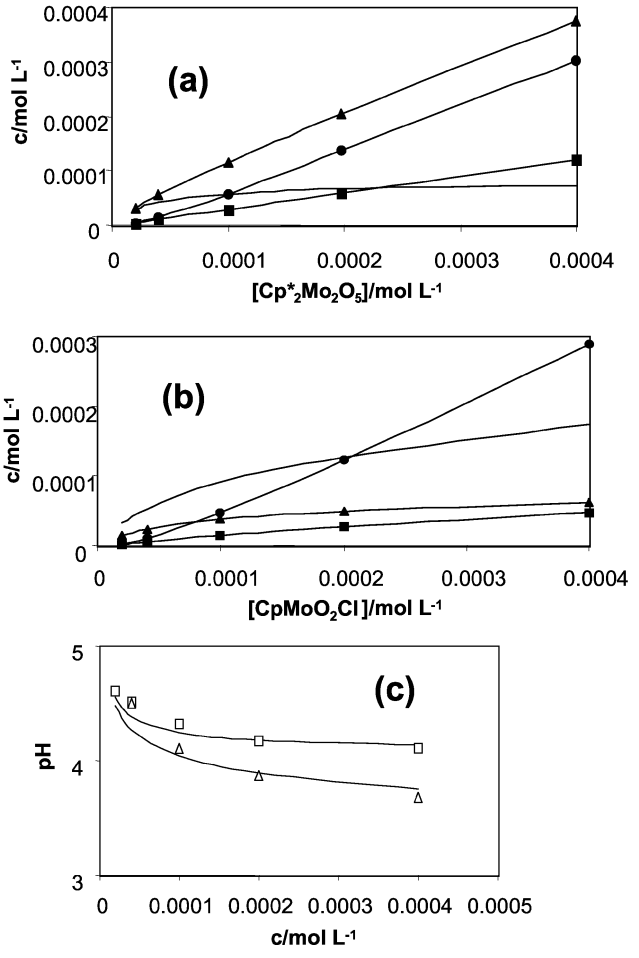

Fig. 8 Calculated concentrations of H^+ (line only), Mo^+ (circles), MoO^- (triangles) and MoOH (squares) for solutions of $Cp^*_2Mo_2O_5$ (*a*) and Cp^*MoO_2Cl (*b*) in 20 : 80 MeOH–H_2O. (*c*) Measured (squares: $Cp^*_2Mo_2O_5$; triangles: Cp^*MoO_2Cl) and calculated (lines) pH as a function of concentration.

(h) The equilibration rate at intermediate pH: general acid-base catalysis

In order to provide an independent verification of the numerical values for all rate constants, kinetic analyses were also attempted in the intermediate pH region. This required the use of a variety of different buffer solutions, as detailed in the experimental section. Given the results outlined in the previous section, we were obviously expecting to obtain overall equilibration rate constants k_{obs} along the theoretical curve shown in Fig. 2. As already mentioned, the transformations were found to follow perfect first-order kinetics under all conditions, including the equilibrium region (2 < pH < 6).

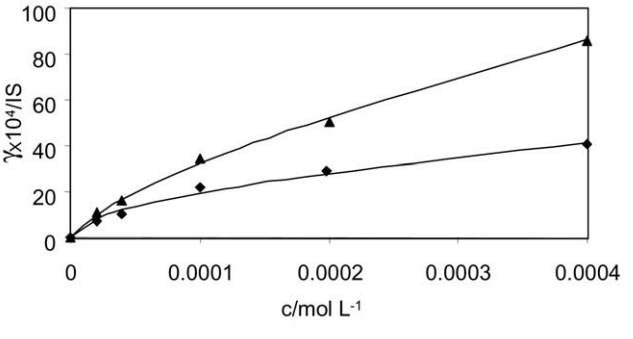

Fig. 9 Measured and calculated conductivity in a 20 : 80 MeOH–H_2O solution as function of the initial concentration for $Cp^*_2Mo_2O_5$ (diamonds) and Cp^*MoO_2Cl (triangles).

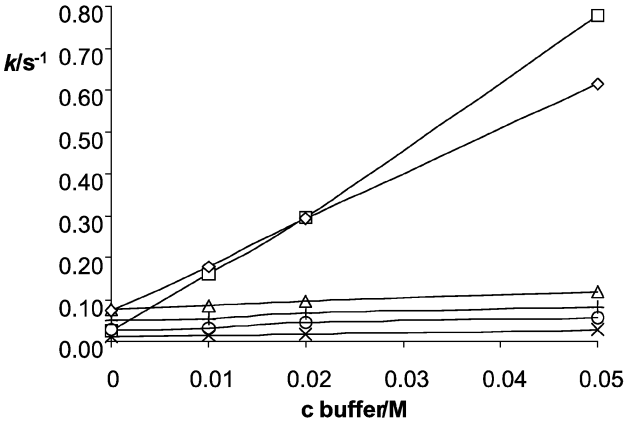

Fig. 10 First-order equilibration constants k_{obs} as a function of buffer concentration at constant pH. Squares: TRIS (pH 7.97); diamonds: borax (pH 9.24); triangles: hydroxylamine (pH 6.34); +: chloroacetic acid (pH 3.01); circles: formic acid (pH 3.77); ×: acetic acid (pH 5.87).

However, the observed values of the first-order rate constants turned out to be infallibly greater than expected. This phenomenon may be attributed to a general acid-base catalysis operated by the buffer's undissociated acid(s) and/or its(their) conjugate base(s). Hydrogen bonding interactions between an undissociated acid and MoOH and $MoOH_2^+$ make the ligands OH^- and H_2O, respectively, better living groups, while the same kind of interactions between the buffer conjugate base and free water molecules or OH^- ions make these better nucleophiles.

This state of affairs is unambiguously proven by detailed studies at different buffer concentrations while keeping the pH and metal concentration constant. Examples are shown in Fig. 10. At each given pH value, the extrapolation of the rate constants to a zero buffer concentration should afford a value in agreement with our developed scheme. This expectation is indeed verified for the experiments at pH 7.97 (TRIS) and 9.24 (borax), see Fig. 2. In other cases, on the other hand, the extrapolation to zero buffer concentration is not sufficiently precise, or the extrapolated value remains significantly higher than the value that is predicted by our scheme. The latter phenomenon occurs in particular within the pH range 2–6. We speculate that this may be caused by the presence of significant equilibrium amounts of compound $Cp^*MoO_2(OH)$, acting itself as a general acid-base catalyst.

(i) Nature of the $MoOH_2^+$ and Mo^+ species

Two different tautomeric forms can be conceived for the $Cp^*MoO_3H_2^+$ ion, namely an aquo-dioxo and a dihydroxo-oxo form, see **I** and **II**. Although the water elimination process requires transit through form **II**, the most stable species may be either one of these two forms. The precise proton distribution for many inorganic aqua ions of molybdenum does not seem to be established with certainty.[36] For instance, compound "MoO_3" is often written as either $Mo(OH)_6$ or $MoO_2(OH)_2(H_2O)_2$. However, if we assume that all proton transfer processes are extremely fast, then the possible involvement of an equilibration between the two tautomers would not affect the rate law of the overall transformation, no matter which of the two is the more stable species.

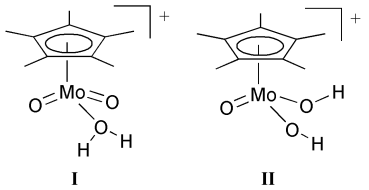

I **II**

The nature of the Mo^+ species also warrants a brief discussion. We have so far assumed that the slow process generating the low pH species is water loss, under the assumption that the proton transfer leading from **I** to **II** is a very rapid process. The loss of bonding to the H_2O molecule would be compensated at least partially by an increase of O-to-Mo π donation. The kinetic data, however, would also be consistent with a slow proton transfer step, in which case the final product could be the water adduct with structure **II**. At this moment, we cannot exclude either possibility. Efforts to isolate a stable salt of this cationic complex, as well as detailed spectroscopic studies in solution, are currently underway in our laboratory. It is important to underline, however, that all the experimental results obtained in this study (kinetic, thermodynamic, conductivity, pH) are unaffected by the solvation state of this ion.

It is possible to find a parallel between the aqueous chemistry of Cp^*Mo^{VI} and that of inorganic molybdenum, when we notice that the $(Cp^{*-})Mo$ unit is isoelectronic with the $Mo(H_2O)_3$ or with the $Mo(H_2O)_2(OH^-)$ units. Thus, compound $Cp^*_2Mo_2O_5$ has a parallel in complex $[Mo_2O_4(\mu\text{-}O)(H_2O)_6]^{2+}$, while compound $Cp^*MoO_2(OH)$ has parallels in complexes $MoO_2(OH)(H_2O)_3^+$ and $MoO_2(OH)_2(H_2O)_2$.[36] The "unsaturated" complex $Cp^*MoO_2^+$ would be related to a species such as $MoO_2(OH)(H_2O)_2^+$ or $MoO_2(H_2O)_3^{2+}$. Like the proton distribution discussed above, the precise hydration level is often unclear for molybdenum aqua ions.[36] While aqueous "MoO_3" is believed to adopt 6-coordination as mentioned above, its conjugate base is usually written as $HMoO_4^-$ [this obviously referring to a 4-coordinate $MoO_3(OH)^-$ complex] and the corresponding dianion MoO_4^{2-} is believed to be 4-coordinate.

Conclusions

The present investigation has unraveled the speciation of the Cp^*Mo^{VI} unit over the entire pH range in an essentially pure aqueous environment. The presence of 20% methanol is necessary to avoid the precipitation of neutral $Cp^*_2Mo_2O_5$ but does not directly participate in the speciation equilibria. The study has revealed the existence and stability as a function of pH of the hitherto unreported complexes $Cp^*MoO_2(OH)$ and $Cp^*MoO_2^+$. In addition, the involvement of a complex having formula $Cp^*MoO_3H_2^+$ as an intermediate in the generation of $Cp^*MoO_2^+$ at low pH has been evidenced by the kinetic studies.

A parallel has been established between the aqueous behavior of Cp^*Mo^{VI} and inorganic Mo^{VI}. An important difference, however, is related to the inertness of the Cp*–Mo bond, which resists hydrolysis down to pH 0. This has the consequence of blocking three coordination positions, rendering the Cp^*Mo^{VI} species unable to form extended oligonuclear aggregates. Aqueous inorganic Mo^{VI}, on the other hand, forms a large variety of polyoxomolybdate ions in the pH range 2–5.[36] As a result, the speciation of Cp^*Mo^{VI} is relatively simple. The results presented in this contribution assist us in the interpretation of the reductive chemistry and electrochemistry of Cp^*Mo^{VI} in an aqueous environment, which is presented in another contribution.[37]

Acknowledgements

We are grateful to the Ministère de la Recherche and to the CNRS for general support through UMR 5632, and to the Conseil Régional de Bourgogne for providing part of the funds for the purchase of the stopped-flow apparatus.

References

1 W. A. Herrmann, *Comments Inorg. Chem.*, 1988, **7**, 73–107.
2 W. A. Herrmann, *Angew. Chem., Int. Ed. Engl.*, 1988, **27**, 1297–1313.
3 W. A. Herrmann and F. E. Kühn, *Acc. Chem. Res.*, 1997, **30**, 169–180.
4 M. Cousins and M. L. H. Green, *J. Chem. Soc.*, 1964, 1567–1572.
5 M. Cousins and M. L. H. Green, *J. Chem. Soc. (A)*, 1969, 16–19.
6 M. J. Bunker and M. L. H. Green, *J. Chem. Soc., Dalton Trans.*, 1981, 847–851.
7 D. Saurenz, F. Demirhan, P. Richard, R. Poli and H. Sitzmann, *Eur. J. Inorg. Chem.*, 2002, 1415–1424.
8 P. Gomez-Sal, E. de Jesus, P. Royo, A. Vazquez de Miguel, S. Martinez-Carrera and S. Garcia-Blanco, *J. Organometal. Chem.*, 1988, **353**, 191–196.
9 J. W. Faller and Y. Ma, *J. Organometal. Chem.*, 1988, **340**, 59–69.
10 P. Leoni, M. Pasquali, L. Salsini, C. di Bugno, D. Braga and P. Sabatino, *J. Chem. Soc., Dalton Trans.*, 1989, 155–159.
11 A. L. Rheingold and J. R. Harper, *J. Organometal. Chem.*, 1991, **403**, 335–344.
12 M. S. Rau, C. M. Kretz, L. A. Mercando, G. L. Geoffroy and A. L. Rheingold, *J. Am. Chem. Soc.*, 1991, **113**, 7420–7421.
13 J. Sundermeyer, U. Radius and C. Burschka, *Chem. Ber.*, 1992, **125**, 2379–2384.
14 M. S. Rau, C. M. Kretz, G. L. Geoffroy and A. L. Rheingold, *Organometallics*, 1993, **12**, 3447–3460.
15 K. Umakoshi and K. Isobe, *J. Organometal. Chem.*, 1990, **395**, 47–53.
16 M. Herberhold, W. Kremnitz, A. Razavi, H. Schöllhorn and U. Thewalt, *Angew. Chem., Int. Ed. Engl.*, 1985, **24**, 601–602.
17 K. Isobe, S. Kimura and Y. Nakamura, *J. Organometal. Chem.*, 1987, **331**, 221–228.
18 F. Bottomley and J. Chen, *Organometallics*, 1992, **11**, 3404–3411.
19 M. S. Rau, C. M. Kretz, G. L. Geoffroy, A. L. Rheingold and B. S. Haggerty, *Organometallics*, 1994, **13**, 1624–1634.
20 M. A. Paul and F. A. Long, *Chem. Rev.*, 1957, **57**, 1–45.
21 The B.R. buffers were solutions of acetic, orthophosphoric, or boric acid partially neutralized with NaOH and containing $NaNO_3$.
22 J. Costa, R. Delgado, M. G. B. Drew, V. Felix and A. Saint-Maurice, *J. Chem. Soc., Dalton Trans.*, 2000, 1907–1916.
23 R. G. Bates, *Determination of pH: Theory and Practice*, John Wiley & Sons, 1965.
24 E. Bosch, P. Bou, H. Allemann and M. Roses, *Anal. Chem.*, 1996, 3651–3657.
25 C. H. Rochester, *J. Chem. Soc., Dalton Trans.*, 1972, 5–8.
26 R. G. Bates, L. Johnson and R. A. Robinson, *Chem. Anal. (Warsaw)*, 1972, **17**, 479–487.
27 A. Liberti and T. S. Light, *J. Chem. Educ.*, 1962, **39**, 236–239.
28 R. A. Binstead, B. Jung and A. D. Zuberbühler, Specfit/32, 2000, Spectrum Software Associates, 2000.
29 R. de Levie, *J. Chem. Educ.*, 1999, **76**, 1594–1598.
30 The formation of $Cp^*MoO_3^-$ is in fact essentially quantitative at $pH > 6$, while the formation of the low pH species is essentially quantitative at $pH < 3$. The kinetics studies in sections a and b have been limited to $pH > 7$ and < 2, respectively, for reasons that will become clear in section g.
31 J. F. Ojo, R. S. Taylor and A. G. Sykes, *J. Chem. Soc., Dalton Trans.*, 1975, 500–505.
32 The nomenclature for the rate constants has been chosen as follows: all k_+ constants correspond to addition of oxygen species (H_2O or OH^-), all k_- to loss of oxygen species; the subscript 1 corresponds to gain/loss of one proton, the subscript 2 to gain/loss of two protons.
33 The difference is attributable to the presence of a small amount of $Cp^*MoO_2(OH)$ at equilibrium, see section h.
34 W. J. Geary, *Coord. Chem. Rev.*, 1971, **7**, 81–122.
35 G. J. Janz and R. P. T. Tomkins, *Nonaqueous Electrolyte Handbook*, Academic Press, New York, 1972.
36 D. T. Richens, in *The Chemistry of Aqua Ions*, J. Wiley & Sons, Chichester, 1997, pp. 259–336.
37 J. Gun, A. Modestov, O. Lev, D. Saurenz, M. Vorotyntsev and R. Poli, submitted for publication.